

. . . , . . .

, 15, 49005, ; e-mail: ai2325434@gmail.com

Fluent SST k- Ansys 20°

This article is devoted to a numerical simulation of the flow in a jet mill ejector equipped with a gas flow control element. This element is a channel wherefrom an additional gas flow enters the accelerating tube of the ejector. The gas flows in the mill ejector are controlled using the energy of additional gas flows, thus increasing the velocity of the main flow at the outlet of the ejector accelerating tube and producing a protective layer around the tube walls to prevent their wear. At the same time, there is no substantiation for the choice of optimal control parameters, a methodology, or scientific methods for gas flow control in the ejector channels. The purpose of this work is to investigate the effect of the location of the gas flow control element on gas-dynamic ejector performance and the flow pattern in the ejector channels. A numerical study was carried out using the Ansys Fluent software package and the SST k- turbulence model. In the course of the study, the pressure of the additional gas flow and the distance from the accelerating tube inlet to the energy carrier supply channel were varied. The angle of the additional gas flow was 20 °. The numerical simulation gave flow patterns in the ejector as a function of the location of the gas flow control element. Streamlines of the additional gas flow were constructed. The article presents the average flow velocity at the accelerating tube outlet and the energy carrier flow rate as a function of the pressure of the additional flow of the energy carrier and the location of the gas flow control element and the maximum values of the average outlet velocity for given pressure ranges. The article substantiates the choice of the gas flow control parameters that maximize the velocity of the mixed flow at the accelerating tube outlet at a minimum gas flow rate. The results may be used in improving material processing technologies.

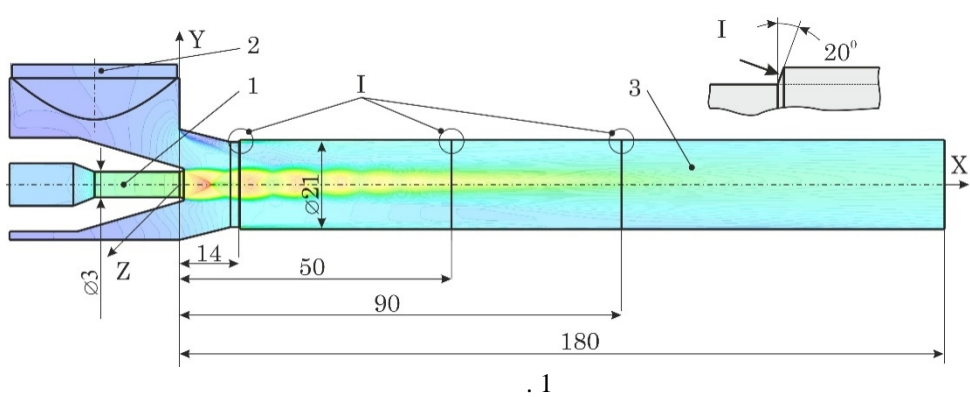
Keywords: control elements, ejector unit, numerical simulation, additional gas flow.

[1] – [3].

© . . . , . . . , 2020

. – 2020. – 3.

1 (), 2 (), 3. () I, 20° (. 1). : $l_{\text{вд}} = 14$, $l_{\text{вд}} = 50$ $l_{\text{вд}} = 90$. 180 .



Ansys Fluent.

60° « » 20°.

[4], [5].

CFD- [6], [7].

[8] – [11], SST $k-\epsilon$.

$k-\epsilon$ $k-\epsilon$ [12].

[13].

SST $k-\epsilon$.

URANS (Unsteady Reynolds Averaged Navier-Stokes – URANS). [14]:

$$\frac{\partial \bar{p}}{\partial t} + \frac{\partial \bar{\rho} \tilde{u}_j}{\partial x_j} = 0,$$

$\rho = \bar{\rho}$, $\rho = \rho_0 / \beta$; $u_j = \tilde{u}_j$, $t = t$, $x_j = x_j$; $j=1,2,3$;

$$\frac{\partial (\bar{\rho} \tilde{u}_i)}{\partial t} + \frac{\partial (\bar{\rho} \tilde{u}_i \tilde{u}_j)}{\partial x_j} = -\frac{\partial P}{\partial x_i} + \frac{\partial (\bar{\tau}_{ij}^{lam} + \bar{\tau}_{ij}^{turb})}{\partial x_j},$$

$i=1,2,3$; $P = \bar{\rho} R \tilde{T}$, $R = R_0 / \beta$, $(\cdot) \cdot \mathbf{K}$, $T = T_0$; $\bar{\tau}_{ij} = \bar{\tau}_{ij}^{lam} + \bar{\tau}_{ij}^{turb}$;

$$\frac{\partial (\bar{\rho} E)}{\partial t} + \frac{\partial ((\bar{\rho} E + P) \tilde{u}_j)}{\partial x_j} = \frac{\partial}{\partial x_j} \left(-q_j^{lam} - q_j^{turb} + \tilde{u}_i (\bar{\tau}_{ij}^{lam} + \bar{\tau}_{ij}^{turb}) \right),$$

$q = -\lambda \frac{\partial \tilde{T}}{\partial x_j}$; $E = \frac{1}{2} \tilde{u}_i \tilde{u}_i + \tilde{T}$;

$$\bar{\tau}_{ji}^{lam} = \mu \left(\frac{\partial \tilde{u}_i}{\partial x_j} + \frac{\partial \tilde{u}_j}{\partial x_i} - \frac{2}{3} \delta_{ij} \frac{\partial \tilde{u}_k}{\partial x_k} \right),$$

$\mu = \mu_0 / \beta$, $\mu_0 = \mu_{ref}$; $k=1,2,3$; $\delta_{ij} = \delta_{ij}$;

$$q_j^{lam} = -\lambda \frac{\partial \tilde{T}}{\partial x_j},$$

$\lambda = \lambda_0 / \beta$, $\lambda_0 = \lambda_{ref}$;

$$\bar{\tau}_{ji}^{turb} = \mu_t \left(\frac{\partial \tilde{u}_i}{\partial x_j} + \frac{\partial \tilde{u}_j}{\partial x_i} - \frac{2}{3} \delta_{ij} \frac{\partial \tilde{u}_k}{\partial x_k} \right) - \frac{2}{3} \delta_{ij} \bar{\rho} k,$$

$$\frac{2}{3} \delta_{ij} \bar{\rho} k$$

; $\mu_t = \mu_t$, $\mu_t = \mu_{t,ref}$;

$$q_j^{turb} = \lambda_t \frac{\partial \tilde{T}}{\partial x_j},$$

$\lambda_t - \dots, \dots / (\cdot \mathbf{K}).$

\dots

[15]:

$$\mu = \mu_0 \left(\frac{T}{T_0} \right)^{3/2} \frac{T_0 + C}{T + C},$$

$\mu_0 = 1,71 \cdot 10^{-5} \text{ Pa} \cdot \text{s}; C = \dots, T = T_0, T_0 = 273, \mu_0 = \dots, C = 117.$

[16]:

$$\frac{\partial(\rho k)}{\partial t} + \frac{\partial(\rho k u_i)}{\partial x_i} = \frac{\partial}{\partial x_j} \left(\Gamma_k \frac{\partial k}{\partial x_j} \right) + G_k - Y_k + S_k,$$

$$\frac{\partial(\rho \omega)}{\partial t} + \frac{\partial(\rho \omega u_i)}{\partial x_i} = \frac{\partial}{\partial x_j} \left(\Gamma_\omega \frac{\partial \omega}{\partial x_j} \right) + G_\omega - Y_\omega + D_\omega + S_\omega,$$

$k - \dots; \omega - \dots; \Gamma_k, \Gamma_\omega - \dots; G_k, G_\omega - \dots; Y_k, Y_\omega - \dots; D_\omega - \dots; S_k, S_\omega - \dots$

300

:

-

;

-

;

-

$0,1, 0,12, 0,14, 0,16 \dots (p_{\text{atm}}) \dots 0,4$

Ansys Meshing.

240

0,5

0 500 /

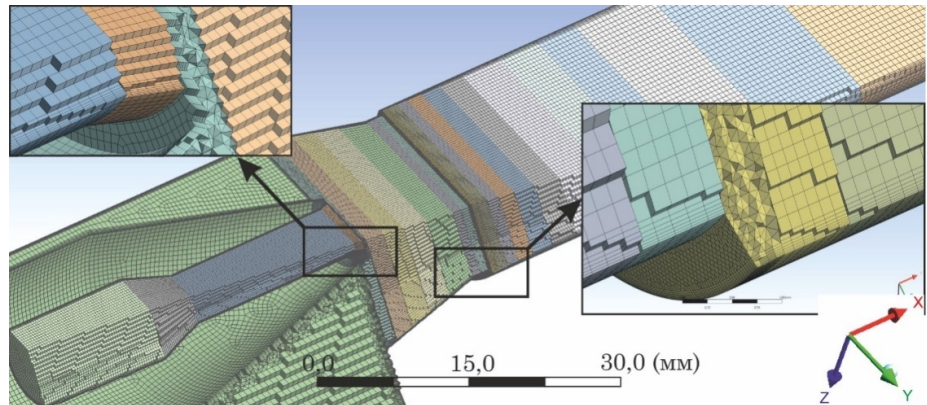
35

Multizone, Sizing,

Inflation

0,136.

.2



.2

« »

«

»

0,1 %.

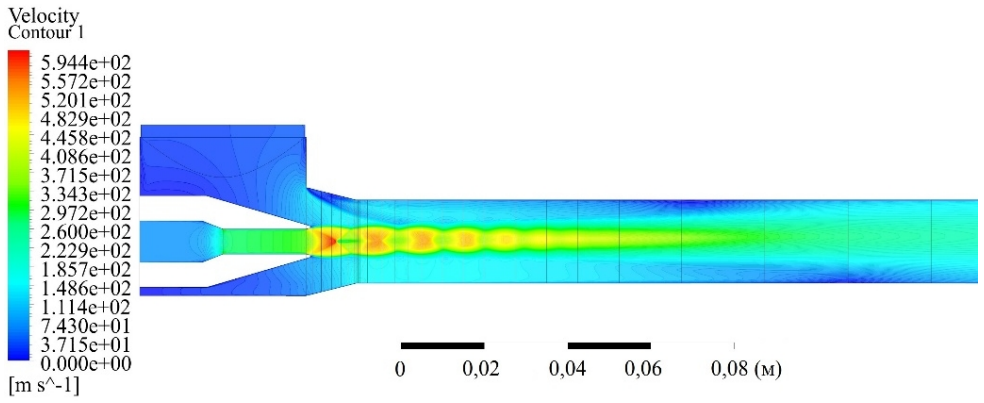
0,0354;

180,85 / .

4,), 4,) – 3

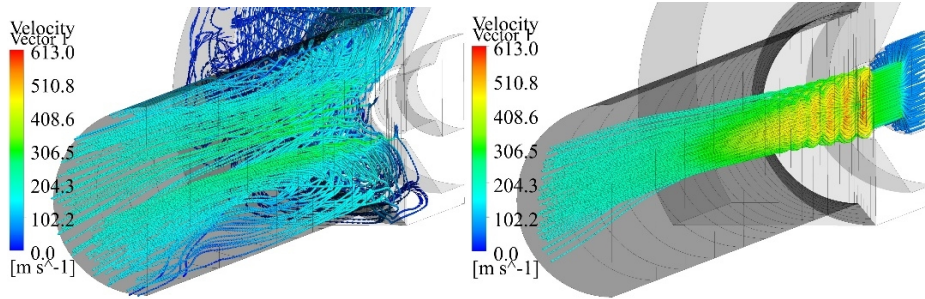
(. 3)

(4 – 5)



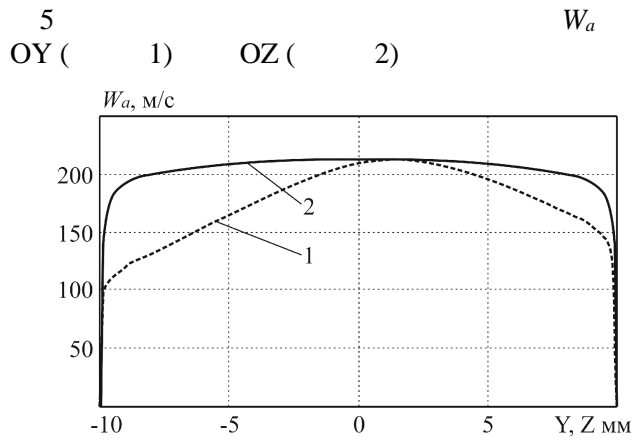
.3

(.4,))
(.4,))



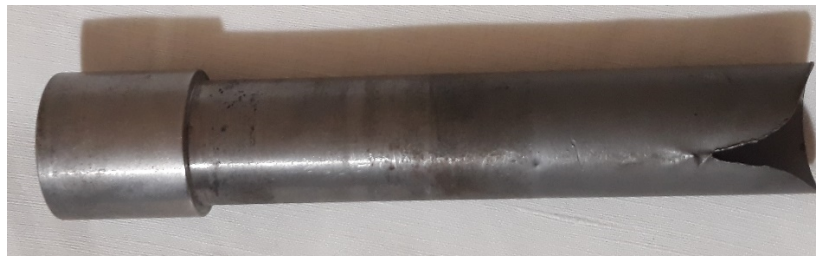
.4

(2 - 3)



.5

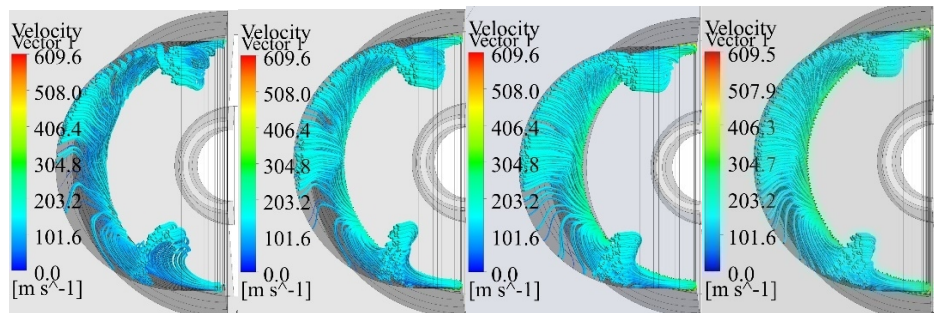
(.6).



.6

« » -

(.7 - .9)
) $p_{e0} = 0,10$;) $p_{e0} = 0,12$;) $p_{e0} = 0,14$;) $p_{e0} = 0,16$
.7
14



))))

.7

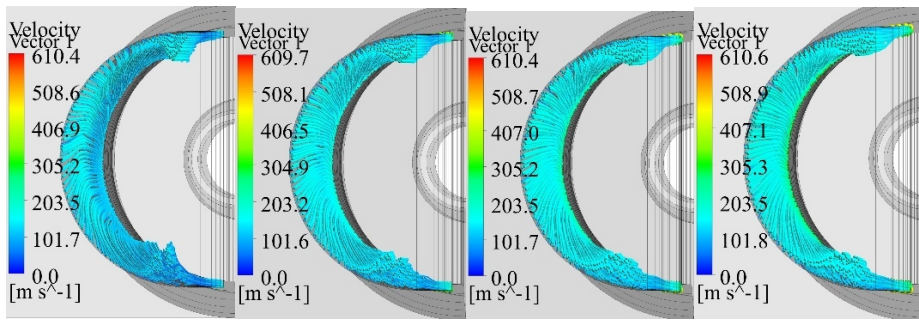
50 (.8,) -))

() .

0,1

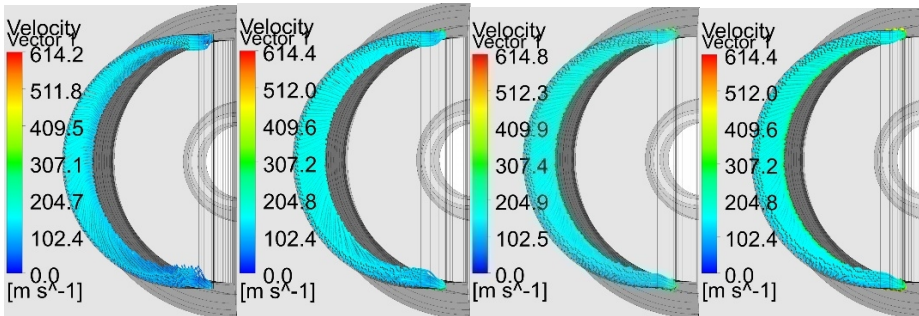
70 - 90 ((3 - 5))

50 (2,5)



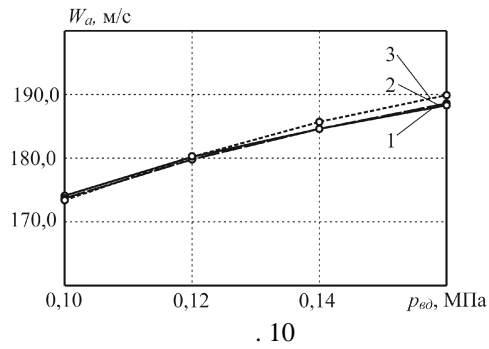
)) .8))

9
90 . 0,1



)) .9))

. 10 : 1 - $X_{\theta 0} = 14$; 2 - $X_{\theta 0} = 50$; 3 - $X_{\theta 0} = 90$.



0,14

. 1.

1 -

		$G_a, /$	$W_a, /$
1	$p_{ед} = 0,10, l_{ед} = 14$	0,0375	174,1
2	$p_{ед} = 0,12, l_{ед} = 14$	0,0389	180,2
3	$p_{ед} = 0,14, l_{ед} = 14$	0,0399	184,6
4	$p_{ед} = 0,16, l_{ед} = 14$	0,0408	188,3
5	$p_{ед} = 0,10, l_{ед} = 50$	0,0373	173,7
6	$p_{ед} = 0,12, l_{ед} = 50$	0,0388	179,8
7	$p_{ед} = 0,14, l_{ед} = 50$	0,0399	184,6
8	$p_{ед} = 0,16, l_{ед} = 50$	0,0409	188,6
9	$p_{ед} = 0,10, l_{ед} = 90$	0,0373	173,4
10	$p_{ед} = 0,12, l_{ед} = 90$	0,0389	180,2
11	$p_{ед} = 0,14, l_{ед} = 90$	0,0402	185,7
12	$p_{ед} = 0,16, l_{ед} = 90$	0,0413	189,9

$G_a -$

$W_a -$

$p_{ед} = 0,10$

1 (180,85 / -

, $p_{ед} = 0,12$

(5 % $p_{ед} = 0,16, l = 90$).

0,393 / .

$p_{e\partial} = 0,14$, $l_{e\partial} = 50$ ($G_a = 0,399$; $W_a = 184,6$ /). , $3 - p_{e\partial} = 0,14$, $l_{e\partial} = 14$ 7 -
 $l_{e\partial} = 14$, -
 $l_{e\partial} = 50$; $p_{e\partial} = 0,14$. , -
 . , -
 .

2 -

1. 2010. . 42. 1. . 65–69. <https://doi.org/10.18372/2306-1472.42.1814>
2. 2010. . XLI, 3. . 69–81. <https://doi.org/10.1615/TsAGISciJ.v41.i3.60>
3. 2019. . 144. . 190–198. <https://doi.org/10.15407/geotm2019.144.190>
4. Huang B., Chang J., Wang C., Petrenko V. A 1-D Analysis of Ejector Performance. Int. J. Refrig. 1999. Vol. 22. No. 5. Pp. 354–364. [https://doi.org/10.1016/S0140-7007\(99\)00004-3](https://doi.org/10.1016/S0140-7007(99)00004-3)
5. Kong F., Kim H. Analytical and Computational Studies on the Performance of a Two-Stage Ejector Diffuser System. Int. J. Heat Mass Transf. 2015. Vol. 85. Pp. 71–87. <https://doi.org/10.1016/j.ijheatmasstransfer.2015.01.117>
6. Gagan J., Smierciew K., Butrymowicz D., Karwacki J. Comparative Study of Turbulence Models in Application to Gas Ejectors. Int. J. Therm. Sci. 2014. Vol. 78. Pp. 9–15. <https://doi.org/10.1016/j.ijthermalsci.2013.11.009>
7. Garcia del Valle J., Sierra-Pallares J., Garcia Carrascal P., Castro Ruiz F. An Experimental and Computational Study of the Flow Pattern in a Refrigerant Ejector. Validation of Turbulence Models and Real-Gas Effects. Appl. Therm. Eng. 2015. Vol. 89. Pp. 795–811. <https://doi.org/10.1016/j.applthermaleng.2015.06.064>
8. Croquer S., Poncet S., Aidoun Z. Turbulence Modeling of a Single-Phase R134a Supersonic Ejector. Part 1: Numerical Benchmark. Int. J. Refrig. 2016. Vol. 61. Pp. 140–152. <https://doi.org/10.1016/j.ijrefrig.2015.07.030>
9. Croquer S., Poncet S., Aidoun Z. Turbulence Modeling of a Single-Phase R134a Supersonic Ejector. Part 2: Local Flow Structure and Exergy Analysis. Int. J. Refrig. 2016. Vol. 61. Pp. 153–165. <https://doi.org/10.1016/j.ijrefrig.2015.07.029>
10. Mazzelli F., Little A.B., Garimella S., Bartosiewicz Y. Computational and Experimental Analysis of Supersonic Air Ejector: Turbulence Modeling and Assessment of 3D Effects. Int. J. Heat Fluid Flow, 2015. Vol. 56. Pp. 305–316. <https://doi.org/10.1016/j.ijheatfluidflow.2015.08.003>
11. Besagni G., Inzoli F. Computational Fluid-Dynamics Modeling of Supersonic Ejectors: Screening of Turbulence Modeling Approaches. Applied Thermal Engineering. 2017. Vol. 117. P. 122–144. <https://doi.org/10.1016/j.applthermaleng.2017.02.011>
12. Menter F. R. Two-Equation Eddy-Viscosity Turbulence Models for Engineering Application. AIAA Journal. 1994. Vol. 32. 8. Pp. 1598–1605. <https://doi.org/10.2514/3.12149>
13. ANSYS 17. . 2017. 210 .
14. Wilcox D. C. Turbulence Modeling for CFD. Griffin Printing. 1993. 460 p.
15. , 1978. 312 .
16. ANSYS Fluent Theory Guide. Release 2019 R1. ANSYS, Inc. 2019. 922 .

07.09.2020,
21.09.2020